



An FFT Computation Minimisation for an FPGA-Based MCSA while Preserving Frequency Resolution

Marut Raksa*, Thanaporn Likitjarernkul, Kiattisak Sengchuai, Nattha Jindapetch and Krerkchai Thongnoo

Department of Electrical Engineering, Faculty of Engineering, Prince of Songkla University, Hat Yai, Songkhla 90112, Thailand

ABSTRACT

This paper presents an FFT computation minimisation for Motor Current Signature Analysis (MCSA) by reducing sampling frequencies and input data samples. The frequency resolution of an FFT signal depends on the FFT length and the sampling frequency. A diagnosis of the induction motor stator winding short turn using the FFT- based MCSA has shown the performance of various FFT lengths. Preserving frequency resolution is achieved by keeping the same ratio of the sampling frequency to the FFT length. From the experimental results, the FFT length can be decreased from 64K to 8K, 1K, and 512 points respectively. All FFT processors were implemented with Xilinx Spartan-6 FPGA to compare the resource, the speed, and the power consumption. The FPGA implementation of the 512-point FFT achieved BRAM saving of 97 %, slice saving of 26%, power consumption saving of 20% and speed up to 187 times compared with the 64K-point FFT. Although the processing gain of the 512-point FFT is 24 dB and decreased from 48.1 dB in the case of the 64K-point FFT, it is enough to classify the short turn fault.

Keywords: FFT; MCSA; Sampling Frequency; Computation Reduction; FPGA

ARTICLE INFO

Article history:

Received: 24 August 2016

Accepted: 03 Jun 2017

E-mail addresses:

marut.r@rmutsv.ac.th (Marut Raksa),

l.thanapond@gmail.com (Thanaporn Likitjarernkul),

ak.kiattisak@hotmail.com (Kiattisak Sengchuai),

nattha.s@psu.ac.th (Nattha Jindapetch),

krerkchai.t@psu.ac.th (Krerckchai Thongnoo)

*Corresponding Author

INTRODUCTION

Fast Fourier Transform (FFT) is widely used in many digital signal processing and communications applications. Especially, the FFT-based MCSA is also effectively used for monitoring failure of induction motors from current signals (Cabal-Yepez, Osornio-Rios, Romero-Troncoso, Razo-Hernandez, & Lopez-Garcia, 2009). The MCSA diagnosis systems have the advantage of easy detection in induction motors. Rangel-Magdaleno, Peregrina-Barreto, Ramirez-Cortes, Gomez-

Gil, & Morales-Caporal.(2014) had proposed a broken bars fault detection of the induction motor, and the method has been implemented in an FPGA to be used in real-time. FPGA-based MCSA implementation is limited by memory for storing input data samples (Pineda-Sanchez et al., 2013). The MCSA needs high-frequency resolution for analysis of the slip frequency neighbouring harmonic frequency (Panigrahy, Konar, and Chattopadhyay, 2014). The slip frequency and the low amplitude of the current spectrum components are related to the fault (Zouzou, Sahraoui, Ghoggal, & Guedidi, 2010). In addition to this, if the induction machine runs on short turn conditions, the amplitude of slip frequencies which depend on the value of the currents, provides very low signal to noise ratio. The simplest way for solving the problem is to use a high-gain FFT processor (Iglesias, Grajal, Sánchez, & López-Vallejo, 2015).

However, a high-gain FFT processor and a high-resolution FFT need long FFT length, which suffers from long computation time and resources as well as power consumption. The FFT length is the number of samples of motor current signals that depend on the sampling frequency and the time that is used to collect the signals. Higher sampling frequency gives a large number of samples. Consequently, a large number of the sample requires a large FFT length processor.

This paper proposes a minimisation of FFT processing by reducing the sampling frequency and input data samples on motor current signature analysis. The frequency resolution is preserved by keeping the same ratio of the sampling frequency to the FFT length. The FPGA implementations of 64K, 8K, 1K, and 512 points-FFT processors for an MCSA diagnosis of the induction motor stator winding short turn have been demonstrated to show reduction in terms of area, speed, and power consumption.

This paper is organised as follows: The first section introduces FFT, while subsequent sections discuss MCSA spectrum measurement, experimental setup, FPGA implementation and results respectively. The final section is the conclusion.

Nomenclature	
N	Size of FFT
X(k)	The FFT output data
n	Integer Number (1, 2, 3...)
K	Odd Harmonic Order
f	Fundamental Frequency (50 HZ)
f_s	Sampling Frequency
f_r	FFT Frequency Resolution
f_{st}	Slip Frequency

FAST FOURIER TRANSFORM

The Fast Fourier Transform provides a divide and conquer method to estimate the Discrete Fourier Transform (DFT) algorithm. The FFT is an efficient algorithm for computing the DFT. In computing, time for a DFT depends on the number of multiplications and input data N

points. The DFT requires N^2 multiplications whereas FFT requires only $N \log_2(N)$. The FFT algorithm is the realisation that a DFT of a sequence of N points can be written in odd and even of length $N/2$. Using the symmetric property of the twiddle factor, (1) can be rewritten to (2), and we can save a lot of computation.

$$X[k] = \sum_{n=0}^{N-1} x[n] e^{-j\left(\frac{2\pi k}{N}\right)n}, k = 0, 1, \dots, N-1, \tag{1}$$

$$X[k] = \sum_{\substack{n=0 \\ \text{even } n}}^{N-1} x[n] e^{-j\left(\frac{2\pi k}{N}\right)n} + \sum_{\substack{n=0 \\ \text{odd } n}}^{N-1} x[n] e^{-j\left(\frac{2\pi k}{N}\right)n} \tag{2}$$

when N is a power of two, and $x(n)$ is an input, $k=0, 1 \dots N-1, f_s$ is a sampling frequency. The frequency resolution of the N -point FFT is determined by (3).

$$f_r = \frac{f_s}{N} \tag{3}$$

The FFT processing gain represents the signal to noise level and can be calculated by (4).

$$FFT_{gain}[dB] = 10 \log\left(\frac{N}{2}\right) \tag{4}$$

The signal to noise in an FFT is low when N is reduced. This affects the measurement of low harmonic signals, such as the frequency of the component of interest or noise.

Nyquist Frequency

The Nyquist frequency is the FFT bandwidth of a sampled signal and is equal to half the sampling frequency of that signal. The sampling frequency is the frequency of the signal at any time. Digital signals must be converted to maximum frequency of the signal frequencies. If the sampling frequency is less than the Nyquist frequency, it will result in signal loss. The FFT bandwidth is defined by (5).

$$FFT_{BW} = \left(\frac{f_s}{2}\right) \tag{5}$$

A suitable N may be selected based on the desired frequency resolution, but it may be impossible to implement on a DSP device. The frequency resolution can be explained as the lowest frequency of the signal that can be described by the FFT, and is given certain as the sampling frequency divided by N (3). Table 1 shows the frequency resolution comparison with different sampling frequencies. The sampling frequency increases from 1 kHz, 5 kHz, and 10 kHz. The FFT frequency resolution is dependent on the sampling frequency of the input signals. For Table2, the sampling frequency of the signal is 1 kHz

It is important to note that at a sampling frequency, increasing the frequency resolution decreases time resolution. That is more accurate in measuring the frequency domain, and less accurate for the time domain. We lose all time information inside the FFT length.

Table 1
Frequency resolution comparison with difference sampling frequency

Sampling Frequency (Fs)	Samples (N)	Data collect time (Sec.)	bins(Fs/N)(Hz)
1kHz	1000	1	1
5kHz	1000	0.5	5
10kHz	1000	0.1	10

Table 2
Frequency resolution comparison with difference sample (N)

Sampling Frequency (Fs)	Samples (N)	Data collect time (Sec.)	bins (Fs/N)(Hz)
6kHz	1000	0.6	6
6kHz	6000	1	1
6kHz	60,000	10	0.1

THE MCSA SPECTRUM MEASUREMENT

The following example illustrates some of the practical issues of signal spectrum frequency measurements. Figure 1 shows the amplitude spectrum of an MCSA signal that has many frequency components. The frequency of the component of interest range is $f_{st\ min}$ to $f_{st\ max}$

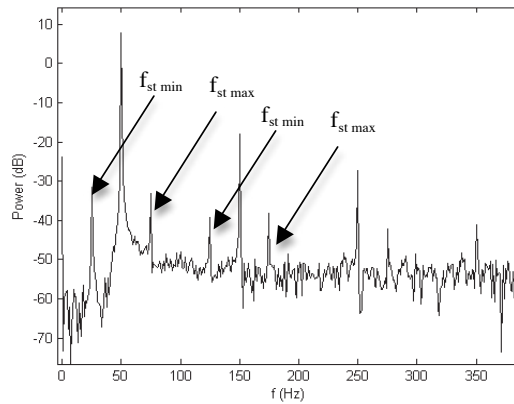


Figure 1. Motor Signature Current (shorted-turn) spectrum frequency

The MCSA is an online tool to detect the fault of stator current and it can detect many faults in the motor such as rotor faults, short turn, bearing faults, and lubrication loss. The frequency spectrum of the MCSA is used to classify the characteristics of short-turn stator faults. The frequency of the induction motor stator winding short turn fault can be calculated by (6).

$$f_{st} = f \left[\frac{n}{p}(1-s) \pm k \right] \tag{6}$$

when Nf is a fundamental frequency, k is a harmonic order, p is pole-pairs and s is a slip of the motor. The stator current signals can be selected to the FFT to extract the frequency components. Each healthy motor gives a certain signature and this signature is affected when faults exist inside the motor. Healthy motors present signature changes when the faults within the motor occur.

EXPERIMENTAL SETUP

In this section, MCSA experimental setup for an induction motor running as a short turn fault is shown in Figure 2. Amplitudes shown in this section are calculated using the frequencies determined by (6). Figure 2 shows the general block diagram of MCSA. The current in the stator of the induction motor is sensed by CTs (Current Transformer), sent to the signal converter, and saved in the data collector. Finally, the computer program identifies the condition of the motor. Its main purpose is to monitor the current of the three-phase stator. The analog signal is given to analog to a digital (A/D) converter. The current is sampled by the A/D converter at the predetermined sampling frequency. This is continued for a sampling period which is sufficient to achieve the required FFT.

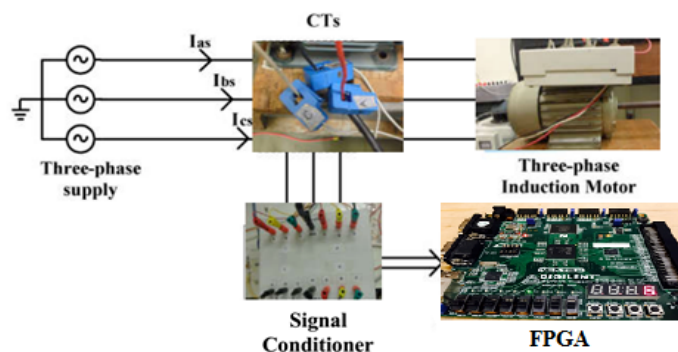


Figure 2. The FPGA based MCSA block diagram

RESULTS AND DISCUSSIONS

From the MCSA as described in the previous section, the values of motor currents are used to perform the FFT and find out the composite harmonics. The motor condition analysis was performed using MATLAB software. The FFT defines harmonic frequency components for an interesting range of magnitudes in different conditions of the motor health. Figure 3 shows the current waveform and the harmonic frequency spectrum of a healthy motor at no load condition.

The current spectrum of the induction motor at the no load condition is shown in Figure 4. In no load scenarios, a speed of the induction motor is 1,495 rpm. When synchronous speed is 1,500 rpm and $s = 0.003$, the slip frequency calculation from (6) is 25 Hz, 75 Hz, 125 Hz and 175 Hz. In full load scenarios, speed of the induction motor is 1,380 rpm and $s = 0.008$. Then the slip frequency is 27 Hz, 73 Hz, 127 Hz and 173 Hz. The current spectrums of the induction motor from no load and full load scenarios are shown in Figure 5.

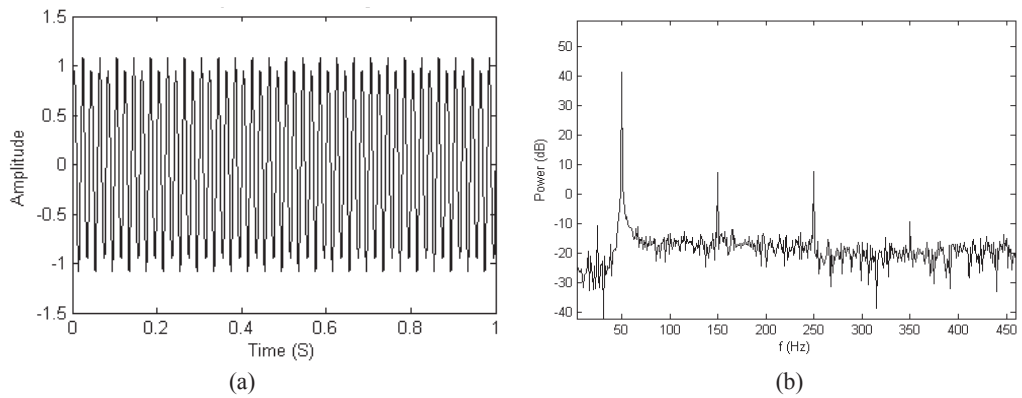


Figure 3. Healthy motor current signal (a) current signal; (b) current spectrum

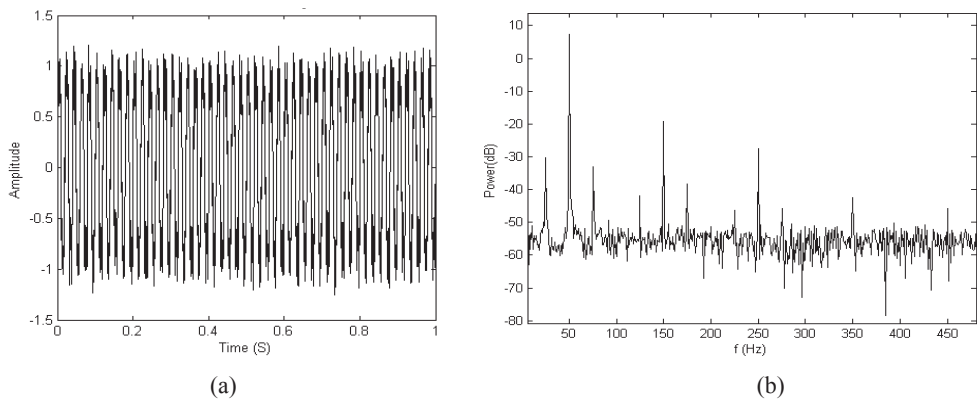


Figure 4. Short turn fault motor current signal (a) current signal ; (b) current spectrum

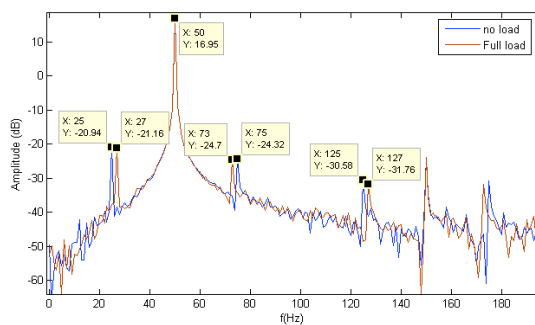


Figure 5. Full load and no load short turn fault current spectrum

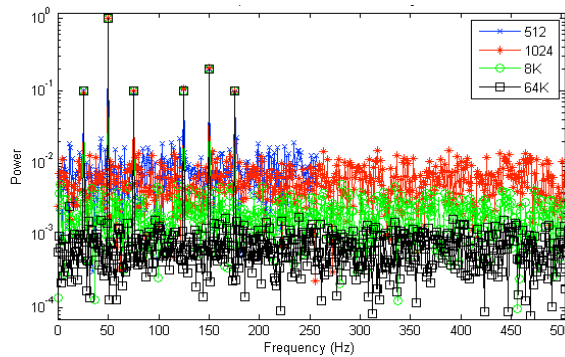


Figure 6. Difference output FFT N= 512, 1k, 8k and 64k from short turn fault motor current signal

Figure 6 shows the current waveform and frequency spectrum of the motor with stator fault (10 turns shorted) at no load condition with FFT N = 512, 1k, 8k, and 64k. The frequency spectrum of the interest range is compared in terms of its length. Observe that FFT N=512 and 64K is different in the signal to noise level. The processing gain of the 512-point FFT is 24 dB, decreased from 48.1 dB in the case of the 64K-point FFT.

FPGA IMPLEMENTATIONS OF FFT

We present four different lengths of FFT processors which apply the radix-2 architecture. The Xilinx System Generator (XSG), which is a high-level graphical programming tool, was used to design a DSP system with the MATLAB Simulink software. The FPGA-based implementations of various FFT processors are summarised in Table 3.

Table 3
A comparison of implementation results using different FFT sizes

FFT size (N)	slice	FFs	BRAMs	LUT	Latency (Clock Cycle)	Power (mW)
512	621	2,734	4	2,010	3,487	36
1,024	979	2,819	6	2,035	7,334	89
8,192	1,284	3,332	34	2,549	96,846	126
65,536	2,358	3,645	244	3,188	655,622	175

All FFT processors were implemented with a Xilinx Spartan-6 FPGA to compare the resource, speed, and power consumption. The FPGA implementation of the 512-point FFT achieved BRAM saving of 97%, slice saving of 26%, FFs saving of 25%, LUT saving of 37%, a power consumption saving of 20% and speed up to 187 times compared with the 64K-point FFT. An FPGA-based can detect short turn fault with different load conditions using MCSA.

CONCLUSION

This paper has discussed an FFT computation minimisation for an FPFA-based MCSA while preserving frequency resolution. It compared frequency spectrum amplitude of outputs with different FFT lengths. The frequency resolution of an FFT signal is dependent on FFT length and sampling frequency. Frequency resolution is preserved by keeping the same ratio of the sampling frequency to the FFT length. Finally, experimental results show the FPGA implementations of the FFT with different lengths. The area, speed and power consumption of the FFT processor depend on the FFT length. The FFT processor gains depend on the FFT length. In this case-study, the 512-point FFT is enough to classify the motor with stator short turn fault.

ACKNOWLEDGEMENT

This work received financial support from the Prince of Songkla University Graduate Studies Grant No. PSU/95000201/2554, Prince of Songkla University (ENG560014S) as well as Center of Excellence in Wireless Sensor Networks (CoE-WSN), Faculty of Engineering, Prince of Songkla University, Hat Yai, Songkhla, Thailand.

REFERENCES

- Cabal-Yepez, E., Osornio-Rios, R. A., Romero-Troncoso, R. J., Razo-Hernandez, J. R., & Lopez-Garcia, R. (2009, December). FPGA-based online induction motor multiple-fault detection with fused FFT and wavelet analysis. In *2009 International Conference on Reconfigurable Computing and FPGAs* (pp. 101-106). IEEE.
- Iglesias, V., Grajal, J., Sánchez, M. A., & López-Vallejo, M. (2015). Implementation of a Real-Time Spectrum Analyzer on FPGA Platforms. *IEEE Transactions on Instrumentation and Measurement*, *64*(2), 338–355.
- Panigrahy, P. S., Konar, P., & Chattopadhyay, P. (2014). Broken bar fault detection using fused DWT-FFT in FPGA platform. In *2014 International Conference on Power, Control and Embedded Systems (ICPCES)* (pp. 1–6).
- Pineda-Sanchez, M., Perez-Cruz, J., Roger-Folch, J., Riera-Guasp, M., Sapena-Baño, A., & Puche-Panadero, R. (2013). Diagnosis of induction motor faults using a DSP and advanced demodulation techniques. In *2013 9th IEEE International Symposium on Diagnostics for Electric Machines, Power Electronics and Drives (SDEMPED)* (pp. 69–76).
- Rangel-Magdaleno, J. de J., Peregrina-Barreto, H., Ramirez-Cortes, J. M., Gomez-Gil, P., & Morales-Caporal, R. (2014). FPGA-Based Broken Bars Detection on Induction Motors Under Different Load Using Motor Current Signature Analysis and Mathematical Morphology. *IEEE Transactions on Instrumentation and Measurement*, *63*(5), 1032–1040.
- Zouzou, S. E., Sahraoui, M., Ghoggal, A., & Guedidi, S. (2010). Detection of inter-turn short-circuit and broken rotor bars in induction motors using the Partial Relative Indexes: Application on the MCSA. In *2010 XIX International Conference on Electrical Machines (ICEM)* (pp. 1–6).